Supplementary Information

Green synthesis of ultra-bright Cs_3MnBr_5 films by CVD method

Shu Li,†[a] Chuanhe Ma,†[a] Fushuai Li,[a] Jinchun Jiang[b] and Hailong Wang*[a]

a. School of Physics and Physical Engineering, Qufu Normal University, Qufu 273165, China. Email:hlwang@qfnu.edu.cn

b. Key Laboratory of Polar Materials and Devices (MOE), Department of Electronic science, East China Normal University,Shanghai 200241,China.

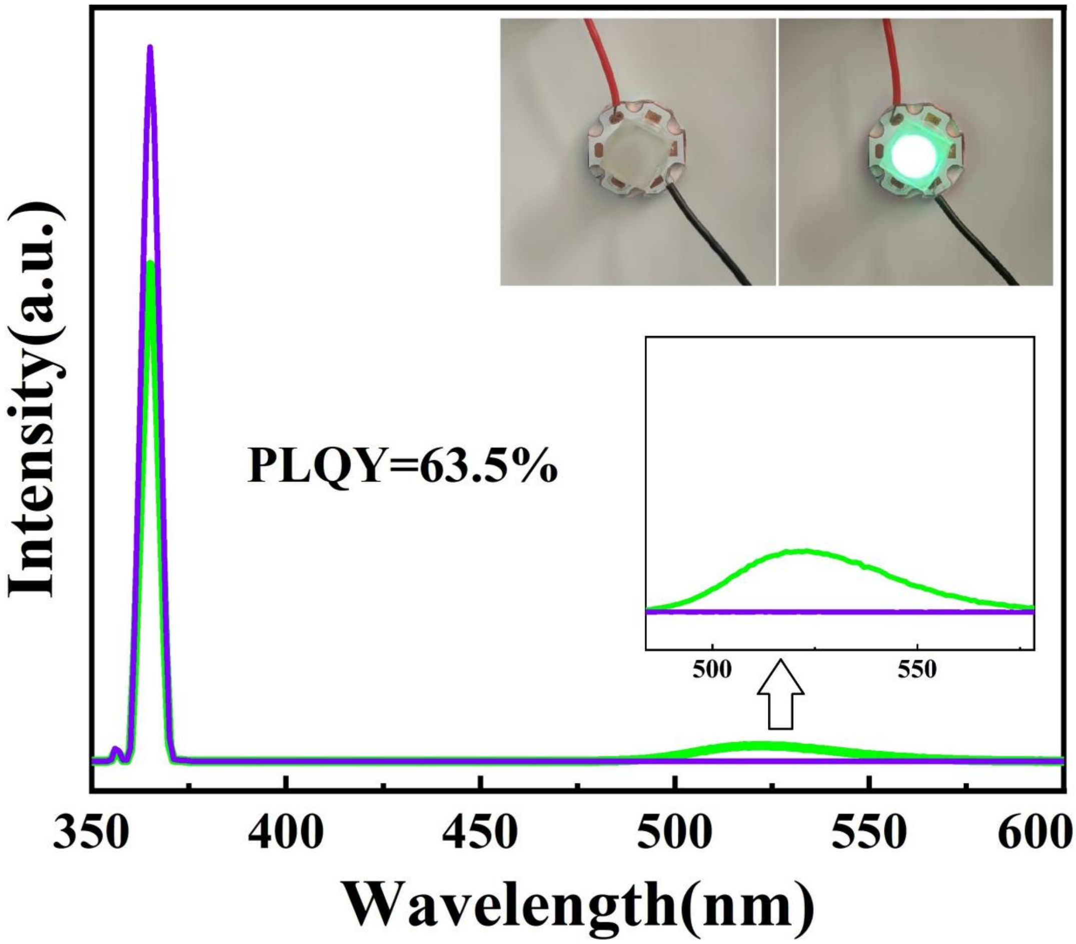

Fig.S1 PLQY of Cs_3MnBr_5 thin film, Inset shows the film being excited by a 365nm LED with and without turning on, respectively

As shown in Fig.S1, the PLQY of Cs_3MnBr_5 film is 63.5%, indicating that this material is ideal for LEDs. We used a 365nm LED chip to pump Cs_3MnBr_5 thin films to demonstrate this application optically. The Cs_3MnBr_5 thin film emits bright green light, proving that it is an ideal candidate for preparing optical devices.

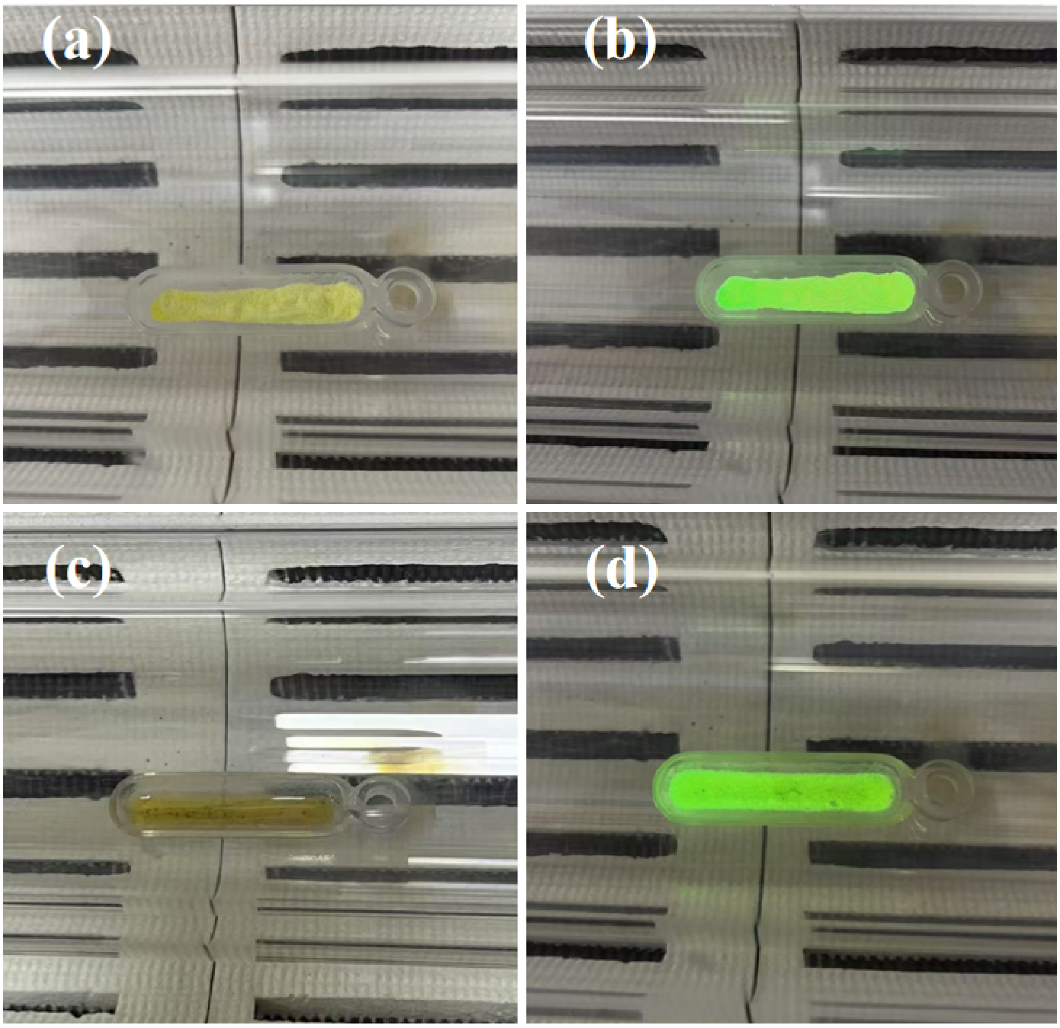

Fig.S2 Physical photos of Cs_3MnBr_5 material at different temperatures, powder at RT before annealing: (a) no excitation light, (b) 365nm excitation light; (c) Melting into liquid at 550 °C; (d) Natural condensation into powder at RT, re-emitting green light under 365nm illumination

To verify that the endothermic extremum at 490 °C in TG and DSC curves is the melting point, we conducted a comparative annealing experiment on the morphology of Cs_3MnBr_5 material. As shown in Fig.S2(a), the Cs_3MnBr_5 material in the quartz boat initially appears as a yellow powder at room temperature. Under 365nm near-infrared light irradiation, Cs_3MnBr_5 powder emits green fluorescence. Our CVD annealing furnace adopts a two-layer quartz tube structure to prevent equipment contamination caused by Cs_3MnBr_5 sublimation. To verify the melting point quickly, considering the temperature gradient field as the thermocouple outside the quartz tube, we directly applied an annealing temperature of 550℃ to Cs_3MnBr_5 powder.

As shown in Fig.S2(c), Cs_3MnBr_5 powder completely melted into a yellow transparent liquid at 550 °C. Therefore, we can conclude that the endothermic extremum at 490 °C in the TG and DSC curves is indeed the melting point. Herein, it is worth pointing out that this is the first disclosure regarding the melting point of Cs_3MnBr_5 powder being around 490 °C. After natural cooling, it is impressive that Cs_3MnBr_5 material can still emit green light, as shown in Fig.S2(d). It indicates that the Cs_3MnBr_5 material we synthesized by CVD method has excellent thermal stability.

Table S1 Comparative analysis of all inorganic lead-free perovskite PLQY and stability

Trans-Temp. denote transition temperature, RT denote room temperature

Materials	Physical form	Emission peak	PLQY	Stability	Ref
$CsCu_2I_3$	Film	548nm	20.6%	PLQY = 95% Init. at 100 ℃	1
$Cs_3Cu_2I_5$	Film	458nm	87%	In 123 phase above 120 ℃	2-3
$CsSnBr_3$	Film	680nm	1.47%（PeLed ）	Oxidation into Sn^{4+} at RT	4
$Cs_3Sb_2Br_9$	QDs	410nm	46%	35 days (70%) at RT	5
$Cs_3Bi_2Br_9$	QDs	468nm	22%	Trans-Temp. is 550 °C	6-7
$Cs_2NaInCl_6$:Yb^{3+}	Crystals	996nm	39.4%	Trans-Temp. is 600 °C	8-9
Cs_2EuCl_6	Nanocrystals	435nm	5.7 ± 0.3%	——	10
Cs_3MnBr_5	Film	520nm	63.5%	Trans-Temp. is 723℃	This Work

We carefully compared and analyzed Cs_3MnBr_5 material with other existing lead-free alternatives, as shown in Table S1, including $CsCu_2I_3$, $Cs_3Cu_2I_5$, $CsSnBr_3$, $Cs_3Sb_2Br_9$, $Cs_3Bi_2Br_9$, $Cs_2NaInCl_6$, and Cs_2EuCl_6. Regarding fluorescence efficiency, $Cs_3Cu_2I_5$ and Cs_3MnBr_5 materials exhibit superior PLQY values. In prior art, the research perspective on lead-free perovskites' temperature stability is inconsistent.

However, together with Fig.7(a) and (b), significant mass loss begins around 723 °C, and the endothermic peak is broad, reaching a minimum weight at 828 °C with a 90% weight loss, indicating sublimation. No significant weight loss occurs below 600°C, indicating excellent thermal stability for our Cs_3MnBr_5 thin films.

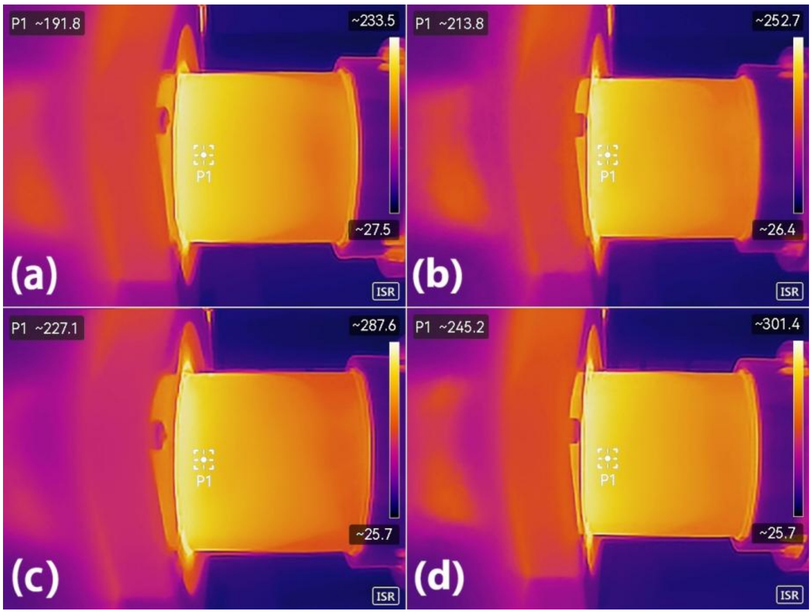

Fig.S3 Temperature Field of CVD Tube Furnace Substrate Side at Different Annealing Temperatures : (a) 700℃, (b) 800℃, (c) 900℃, (d) 1000℃

Temperature critically affects grain size and surface morphology in high-quality perovskite films[11]. Using the H3Pro thermal imager, we measured temperature distribution across the substrate in a tube annealing furnace.

As the annealing temperature at the quartz boat side rose from 700-1000 ℃, the target detects temperatures increase in sequence at the P1 area of the substrate side: 191.8 ℃, 213.8 ℃, 227.1 ℃, and 245.2 ℃. The rise in the highest values and P1 temperatures is mainly due to quartz tube heat conduction and raw material vapor. Determining substrate temperature supports process optimization and high-quality Cs_3MnBr_5 film preparation.

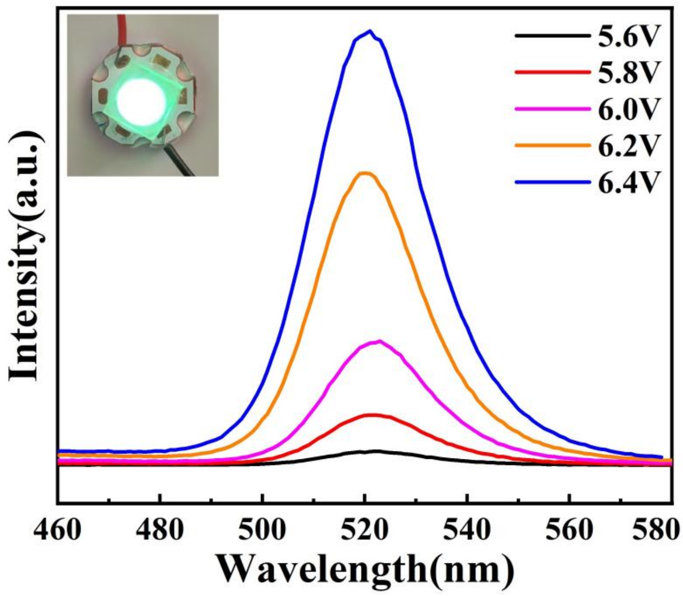

Fig.S4 The PL intensity of Cs_3MnBr_5 LED under different driving voltages

Cs_3MnBr_5, with broadband transmission, high PLQY, and stability, suits solid-state lighting. Figure S4 shows practical PL devices using Cs_3MnBr_5 thin film on a 365nm UV LED chip. PL intensity increases with driving voltage (5.6-6.4V), allowing voltage analysis via light intensity. Fitting its function curve can further analyze the voltage amplitude and stability from the perspective of light intensity.

References

1 Z.Ma, Z. Shi, C. Qin, M. Cui, D. Yang, X. Wang, L. Wang, X. Ji, X. Chen, J. Sun, D. Wu, Y. Zhang, X. J. Li, L. Zhang and C. Shan (2020). ACS Nano 14(4): 4475-4486.

2 T.Chen, X. Li, Y. Wang, F. Lin, R. Liu, W. Zhang, J. Yang, R. Wang, X. Wen, B. Meng, X. Xu and C. Wang (2023). Journal of Energy Chemistry 79: 382-389.

3 W.Cui, J. Zhao, L. Wang, P. Lv, X. Li, Z. Yin, C. Yang and A. Tang (2022). The Journal of Physical Chemistry Letters 13(22): 4856-4863.

4 J.-M.Heo, H. Cho, S.-C. Lee, M.-H. Park, J. S. Kim, H. Kim, J. Park, Y.-H. Kim, H. J. Yun, E. Yoon, D.-H. Kim, S. Ahn, S.-J. Kwon, C.-Y. Park and T.-W. Lee (2022). ACS Energy Letters 7(8): 2807-2815.

5 J.Zhang, Y. Yang, H. Deng, U. Farooq, X. Yang, J. Khan, J. Tang and H. Song (2017). ACS Nano 11(9): 9294-9302.

6 Y.Lou, M. Fang, J. Chen and Y. Zhao (2018). Chemical Communications 54(30): 3779-3782.

7 Y.Zhang, Y. Liu, Z. Xu, H. Ye, Z. Yang, J. You, M. Liu, Y. He, M. G. Kanatzidis and S. Liu (2020). Nature Communications 11(1):2304.

8 S.Han, D. Tu, Z. Xie, Y. Zhang, J. Li, Y. Pei, J. Xu, Z. Gong and X. Chen (2022). Advanced Science 9(32):2203735.

9 R.Zeng, L. Zhang, Y. Xue, B. Ke, Z. Zhao, D. Huang, Q. Wei, W. Zhou and B. Zou (2020). The Journal of Physical Chemistry Letters 11(6): 2053-2061.

10 J.Huang, T. Lei, M. Siron, Y. Zhang, S. Yu, F. Seeler, A. Dehestani, L. N. Quan, K. Schierle-Arndt and P. Yang (2020). Nano Letters 20(5): 3734-3739.

11 S.Li, Y. Xiao, R. Su, W. Xu, D. Luo, P. Huang, L. Dai, P. Chen, P. Caprioglio, K. A. Elmestekawy, M. Dubajic, C. Chosy, J. Hu, I. Habib, A. Dasgupta, D. Guo, Y. Boeije, S. J. Zelewski, Z. Lu, T. Huang, Q. Li, J. Wang, H. Yan, H.-H. Chen, C. Li, B. A. I. Lewis, D. Wang, J. Wu, L. Zhao, B. Han, J. Wang, L. M. Herz, J. R. Durrant, K. S. Novoselov, Z.-H. Lu, Q. Gong, S. D. Stranks, H. J. Snaith and R. Zhu (2024). Nature 635(8040): 874-881.